

University of Kentucky

UKnowledge

---

Chemistry Faculty Publications

Chemistry

---

2-13-2017

## Dual-Functional-Tag-Facilitated Protein Labeling and Immobilization

Xinyi Zhang

*University of Kentucky*, xinyi.zhang@uky.edu

Wei Lu

*University of Kentucky*

Kevin Kwan

*University of Kentucky*, kevin.kwan@uky.edu

Dibakar Bhattacharyya

*University of Kentucky*, db@uky.edu

Yinan Wei

*University of Kentucky*, yinan.wei@uky.edu

Follow this and additional works at: [https://uknowledge.uky.edu/chemistry\\_facpub](https://uknowledge.uky.edu/chemistry_facpub)



Part of the [Amino Acids, Peptides, and Proteins Commons](#), [Cell and Developmental Biology Commons](#), [Chemistry Commons](#), and the [Molecular Biology Commons](#)

[Right click to open a feedback form in a new tab to let us know how this document benefits you.](#)

---

### Repository Citation

Zhang, Xinyi; Lu, Wei; Kwan, Kevin; Bhattacharyya, Dibakar; and Wei, Yinan, "Dual-Functional-Tag-Facilitated Protein Labeling and Immobilization" (2017). *Chemistry Faculty Publications*. 96.  
[https://uknowledge.uky.edu/chemistry\\_facpub/96](https://uknowledge.uky.edu/chemistry_facpub/96)

This Article is brought to you for free and open access by the Chemistry at UKnowledge. It has been accepted for inclusion in Chemistry Faculty Publications by an authorized administrator of UKnowledge. For more information, please contact [UKnowledge@lsv.uky.edu](mailto:UKnowledge@lsv.uky.edu).

---

## Dual-Functional-Tag-Facilitated Protein Labeling and Immobilization

Digital Object Identifier (DOI)

<https://doi.org/10.1021/acsomega.6b00512>

### Notes/Citation Information

Published in *ACS Omega*, v. 2, issue 2, p. 522-528.

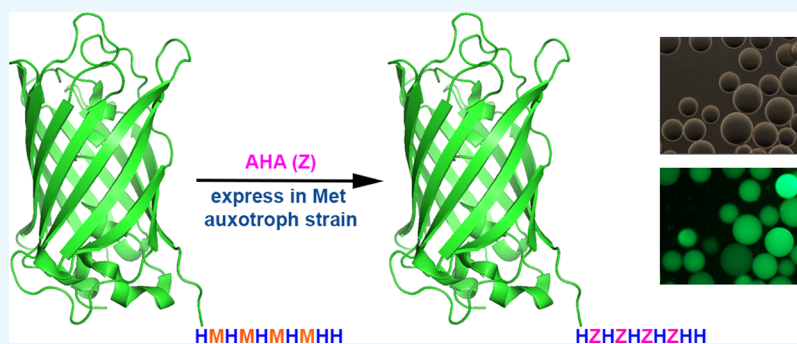
Copyright © 2017 American Chemical Society

This is an open access article published under an ACS AuthorChoice [License](#), which permits copying and redistribution of the article or any adaptations for non-commercial purposes.

# Dual-Functional-Tag-Facilitated Protein Labeling and Immobilization

Xinyi Zhang,<sup>†</sup> Wei Lu,<sup>†</sup> Kevin Kwan,<sup>†</sup> Dibakar Bhattacharyya,<sup>‡</sup> and Yinan Wei<sup>\*,†</sup>

<sup>†</sup>Department of Chemistry and <sup>‡</sup>Department of Chemical and Materials Engineering, University of Kentucky, Lexington, Kentucky 40506, United States



**ABSTRACT:** An important strategy in the construction of biomimetic membranes and devices is to use natural proteins as the functional components for incorporation in a polymeric or nanocomposite matrix. Toward this goal, an important step is to immobilize proteins with high efficiency and precision without disrupting the protein function. Here, we developed a dual-functional tag containing histidine and the non-natural amino acid azidohomoalanine (AHA). AHA is metabolically incorporated into the protein, taking advantage of the Met-tRNA and Met-tRNA synthetase. Histidine in the tag can facilitate metal-affinity purification, whereas AHA can react with an alkyne-functionalized probe or surface via well-established click chemistry. We tested the performance of the tag using two model proteins, green fluorescence protein and an enzyme pyrophosphatase. We found that the addition of the tag and the incorporation of AHA did not significantly impair the properties of these proteins, and the histidine–AHA tag can facilitate protein purification, immobilization, and labeling.

## INTRODUCTION

Proteins are functional materials created by nature to execute diverse activities in living organisms. The superb selectivity, specificity, and performance of proteins have made them highly desirable components in the creation of biomimetic materials. A major obstacle in the utilization of proteins in biotechnology is the difficulty with site-specific immobilization of proteins without compromising their functions. Introduction of a peptide tag has been a popular method to facilitate protein immobilization or detection. Such peptide tags include the GST tag,<sup>1,2</sup> strep tag,<sup>3–5</sup> HA tag,<sup>6,7</sup> flag tag,<sup>8–10</sup> arg tag,<sup>11,12</sup> c-myc tag,<sup>13,14</sup> and His-tag.<sup>15,16</sup> Proteins bearing these tags can be captured or detected via interactions with their corresponding binding-partner modules or antibodies. Peptide tags are usually directly encoded into the gene of the target protein and thus have the advantage of being convenient and highly specific. Although they are very useful in the purification and detection of the tagged proteins, the application of most peptide tags in protein immobilization and modification is limited by the noncovalent nature of the interaction, which suffers from drawbacks including a high off-rate and low mechanical resilience. Several systems have been developed to promote the formation of covalent bonds between a residue in the peptide tag and its catcher module, such as split inteins,<sup>17</sup> the SpyTag/SpyCatcher,<sup>18–20</sup> cysteine and  $\alpha$ -chloroacetyl interaction facilitated by the coil–coil interaction,<sup>21</sup> the His-tag and

nitrilotriacetate-based arylazide photoreactive label via click chemistry,<sup>22,23</sup> and the use of the substrate peptide of a ligase or transferase, such as the LAP tag,<sup>24</sup> the Q tag,<sup>25</sup> the sortagging motif,<sup>26</sup> the formyl glycine tag,<sup>27</sup> and the peptides A1 and S6.<sup>28</sup>

Incorporation of non-natural amino acids is another useful technique used in the site-specific modification of proteins. Examples include the azido- or alkyne-containing residues via click chemistry,<sup>29</sup> norbornene-containing residues that react with tetrazine-based probes,<sup>30</sup> and *p*-azido-*L*-phenylalanine via photocatalytic reaction.<sup>31</sup> Non-natural amino acids are usually introduced into the protein of interest through the introduction of a dedicated orthogonal pair of tRNA and tRNA synthetase that translate a stop codon (typically TAG) into the specific non-natural amino acid. Recently, this method has been coupled with *in situ* biosynthesis to incorporate a sulfur-containing noncanonical amino acid, *S*-allyl-*L*-cysteine, into *Escherichia coli* proteins.<sup>32</sup> Subsequently, the non-natural amino acid can introduce unique chemistry to facilitate site-specific modification. Alternatively, if the structure of a non-natural amino acid is very similar to that of a natural amino acid, it can be incorporated metabolically using the corresponding auxotrophic strain. In this case, no additional cellular

Received: December 15, 2016

Accepted: January 30, 2017

Published: February 13, 2017

machineries need to be introduced. For example, azidohomocysteine (AHA) can be incorporated into the sequence of proteins by Met-tRNA and tRNA synthetase (Figure 1A). This

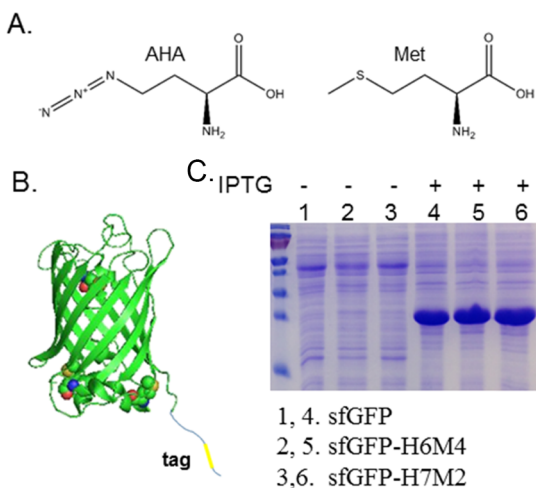


**Figure 1.** (A) Structure of methionine and AHA. (B) Structure of sfGFP with the side chain of the three intrinsic methionine residues highlighted with a ball-and-stick model. The location of the C-terminal tag is shown. (C) Cell lysate of *DL41(DE3)* transformed with the corresponding plasmids before or after IPTG induction. Molecular weights of bands in the marker, from top to bottom, are 130, 100, 70, 55, 40, 35, 25, and 15 kD, respectively.

method has been used by several groups to label and modify proteins.<sup>33–43</sup> However, labeling of the incorporated AHAs often suffers from poor efficiency because methionine residues usually form part of the hydrophobic core of a protein and thus have limited accessibility to reactions. Although all proteins contain methionine (and thus the ATG codon for AHA incorporation) in their amino acid sequences, only a small percentage of these residues seemed to be accessible for labeling. One potential solution is to denature and unfold the target protein before labeling to improve the accessibility of the AHA residues.<sup>29,44</sup> This approach is very useful in the detection of a target protein but not suitable for applications that demand active proteins. Otherwise, the residue can be introduced at the surface of the protein via site-directed mutagenesis.<sup>38</sup> Here, we take advantage of the convenience of metabolic incorporation and address the issue of limited accessibility through the genetic introduction of a tag containing the ATG codon. To avoid the formation of a hydrophobic patch that may potentially affect protein folding, we inserted polar residues (histidine or serine) between neighboring Met/AHA residues. The tag has two functions: histidine in the tag can facilitate protein purification via the conventional metal-affinity chromatography, whereas methionine (or rather, its replacement by AHA) can be used in covalent labeling. The performance of the tags was evaluated using two model proteins, superfolder green fluorescent protein (sfGFP) and inorganic pyrophosphatase from *Staphylococcus aureus* (PpaC).<sup>45</sup> sfGFP was chosen owing to its intrinsic fluorescence, whereas PpaC was chosen because its enzymatic activity can be conveniently measured using a colorimetric assay. Using these two model proteins, we demonstrated that the incorporation of the tag did not compromise the function of proteins, and the tag could facilitate both protein purification and modification. We expect the dual-functional His–AHA tag to be useful in general for various biotechnological applications.

## RESULTS AND DISCUSSION

### Incorporation of AHA into the Target Proteins.

Expression of AHA-containing proteins was performed using a methionine auxotrophic strain, *DL41(DE3)*. *DL41(DE3)* could not grow in the absence of methionine (Figure 2A). The

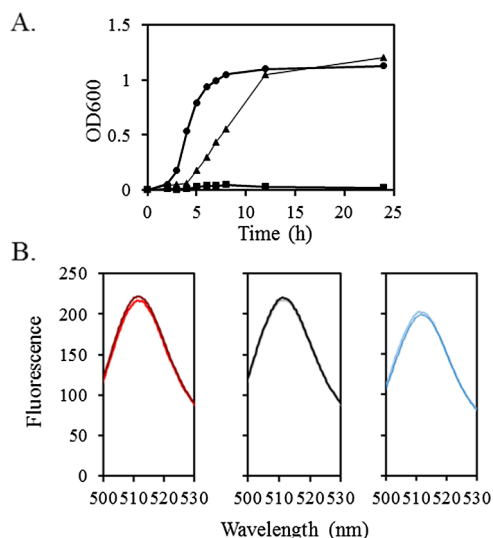


**Figure 2.** (A) *DL41(DE3)* growth curves cultured in M9 medium supplemented with different amino acids: 19 essential amino acids (no methionine) (squares), all 20 essential amino acids (circles), and 19 essential amino acids (no methionine) plus AHA (triangles). (B) Fluorescence spectra of sfGFP-H6 containing methionine (red) or AHA (magenta); sfGFP-H7M2 containing methionine (gray) or AHA (black); and sfGFP-H6M4 containing methionine (blue) or AHA (dark blue).

replacement of Met by AHA slowed down the growth of the strain and increased the doubling time at the exponential growth phase from 1 to 2 h, but the two cultures grew to similar densities at saturation. This result indicates that AHA can be used effectively as a replacement of methionine in the synthesis of proteins and supports cell growth. To further confirm that AHA was incorporated to replace methionine, we submitted AHA-containing PpaC-H6G3M4 (Table 1) for mass spectrometry peptide fingerprinting analysis. There are 13 methionine residues in the protein, including four in the tag. Among them, the peptide containing AHA-substituted Met1, Met125, or M142 was not detected. Peptides containing AHA replacement of all 10 other methionine residues were identified, indicating that these residues were at least partially replaced by AHA.

**Incorporation of a Dual-Functional Tag at the C-Terminus of sfGFP.** The intrinsic fluorescence of sfGFP makes it a popular model protein in studies involving protein modification, including ones using the azido-alkyne-based click chemistry.<sup>50</sup> The polyhistidine tag has been used extensively in the purification of sfGFP.<sup>51</sup> Here, we have tested two different tag designs, with the addition of two or four methionine residues (Figure 1 and Table 1). To avoid the potential creation of a hydrophobic patch, we juxtaposed methionine with histidine. For protein expression, *E. coli* strain *DL41(DE3)* containing the plasmid sfGFP-H6, sfGFP-H7M2, or sfGFP-H6M4 was grown in the M9 medium supplemented with 20 essential amino acids, as described in the Materials and Methods. As shown in Figure 1C, the different tags did not affect the expression level of the protein. The two proteins

Table 1. Primer and Tag Sequences

construct	primers	tag sequence
sfGFP-H7M2	5'-atgcacatgtgagatccggctgctaaca-3' 5'-ggatctcacatgtgcatgtggtggtggtg-3'	HHHHHHMHM
sfGFP-H6M4	5'-catatgcacatgcacatgcactaacggctgctaacaagc-3' 5'-gcatgtgcatgtgcatgtggtggtggtgtagag-3'	HMHMHMHMHH
PpaC-H6GS3M4	5'-gcatgagcatgagcatgtgataatgagatccggctgc-3' 5'-gctcatgctcatgctcatgcatgatggtggtggtgctcgag-3'	HHHHHHGMSMSMSM

containing methionine residues in the tag can be purified similarly as that of the His-tagged sfGFP, with similar yields and purity (data not shown).

To examine the potential effect of the tag and the replacement of methionine by AHA on the protein structure, we measured the fluorescence spectra of the three proteins, sfGFP-H6, sfGFP-H7M2, and sfGFP-H6M4, containing methionine or AHA. After expression and purification, the fluorescence spectra of the protein samples were collected (Figure 2B). Six protein samples were examined, including the three different constructs of sfGFP expressed in the presence of either methionine or AHA. The wavelength of the emission peak was not affected by the addition of the tags or the incorporation of AHA. For each construct, the replacement of methionine by AHA did not affect the fluorescence intensity. The fluorescence intensity of sfGFP-H6M4 was approximately 10% lower than that of sfGFP-H6 and sfGFP-H7M2.

Then, we examined the effect of the Met-containing tag in promoting the efficiency of a click-chemistry reaction. Purified sfGFP bearing H6, H7M2, or H6M4 tag was subjected to labeling using biotin alkyne followed by detection using anti-biotin western blot (WB). As shown in Figure 3A, the level of labeling of sfGFP-H6M4 was significantly better than that of sfGFP-H7M2, which was also better than that of sfGFP-H6. The relative levels of labeling of H6M4 and H7M2 were

approximately 10- and 3-fold, respectively, as the level of sfGFP-H6. There are three intrinsic methionine residues in sfGFP, as highlighted in Figure 1B. The side chain of these methionine residues is likely involved in hydrophobic interactions in the native structure of sfGFP. Therefore, when AHA replaces these methionine residues, its side chains likely have limited accessibility for the reaction.

To demonstrate the usefulness of the tag in facilitating immobilization, we expressed sfGFP-H6M4 in the presence of AHA or methionine and incubated the alkyne agarose resin with purified proteins. After washing, images of the modified resin under normal white light or blue light (Figure 3B,C) were taken. It is clear that the reaction with the alkyne agarose resin depends on the presence of AHA in the protein. The immobilization of AHA-containing sfGFP-H6M4 is highly specific. AHA-containing sfGFP-H6M4 readily attached to the alkyne beads, whereas no binding could be detected for sfGFP-H6M4 expressed in the absence of AHA.

**Addition of the GS3M4 Tag to PpaC.** We used PpaC as a model enzyme to further examine the performance of the methionine-containing tag. Here, we added an octapeptide “GMSMSMSM” after the His-tag at the C-terminus of PpaC (Table 1). PpaC is a good model enzyme because the protein can be expressed and purified at high yields, and its catalytic activity can be measured using a convenient colorimetric assay. We have previously determined the crystal structure of PpaC-H6.<sup>45</sup> It exists as a dimer, and each subunit contains nine intrinsic methionine residues (Figure 4A).

To examine the effect of the tag and the incorporation of AHA on the catalytic activity of PpaC, we first compared the catalytic activity of PpaC-H6 and PpaC-H6GS3M4 expressed in *DL41(DE3)* grown in the presence of methionine (Figure 4B, black and red). The fit to the Michaelis–Menten equation yielded  $K_M$  and  $k_{cat}$  of  $44 \pm 9 \mu\text{M}$  and  $887 \pm 97 \mu\text{mol}\cdot\text{min}^{-1}\cdot\text{mg}^{-1}$ , respectively, for PpaC-H6GS3M4, which are not significantly different from the  $K_M$  and  $k_{cat}$  of PpaC-H6 ( $52 \pm 15 \mu\text{M}$  and  $897 \pm 98 \mu\text{mol}\cdot\text{min}^{-1}\cdot\text{mg}^{-1}$ , respectively). Next, we compared  $K_M$  and  $k_{cat}$  of PpaC-H6GS3M4 expressed with AHA (Figure 4B, red and blue).  $K_M$  and  $k_{cat}$  of the protein expressed from cells grown in the presence of AHA are  $43 \pm 11 \mu\text{M}$  and  $1050 \pm 101 \mu\text{mol}\cdot\text{min}^{-1}\cdot\text{mg}^{-1}$ . Differences in  $K_M$  and  $k_{cat}$  between the AHA-containing PpaC and non-AHA-containing PpaC are not statistically significant.

To compare the level of labeling of PpaC-H6 and PpaC-H6GS3M4, we expressed the two proteins in the presence of AHA as described. Although each PpaC subunit contains nine intrinsic methionine residues, the level of labeling of PpaC-H6 was much lower than the level of labeling of PpaC-H6GS3M4 (Figure 4C). Although similar amounts of proteins were used in the experiment, the band intensity of PpaC-H6GS3M4 in the anti-biotin WB was approximately four times the band intensity of PpaC-H6. In spite of the abundance of the intrinsic

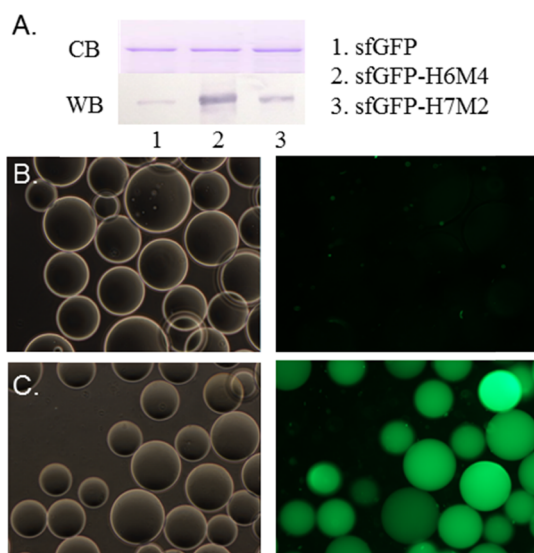


**Figure 3.** (A) Coomassie blue (CB) stain and anti-biotin WB analysis of three AHA-containing sfGFP constructs reacted with biotin alkyne. (B) Alkyne agarose resin incubated with sfGFP-H6M4 expressed with methionine and then imaged using normal white light (left) or blue light (right). (C) Alkyne agarose resin incubated with sfGFP-H6M4 expressed with AHA and then imaged using normal white light (left) or blue light (right).

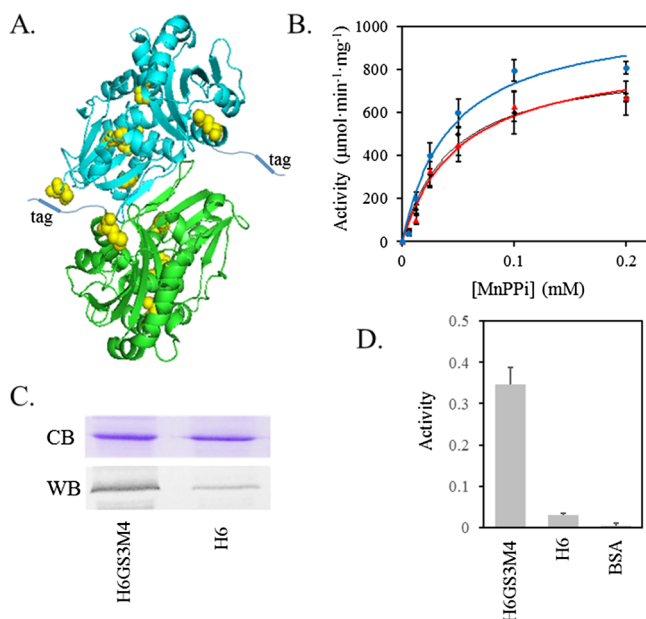


**Figure 4.** Structure, catalytic activity, and labeling of PpaC. (A) Ribbon diagram of the structure of PpaC-H6 (created from 4RPA). The two subunits in the dimer are color-coded. Methionine residues in the structure are highlighted in yellow ball-and-stick models. (B) Michaelis–Menten plot of PpaC-H6 (black), PpaC-H6GS3M4 (red), and PpaC-H6GS3M4 containing AHA (blue). Each experiment was repeated three times. The average value and standard deviations are shown. Data were fitted using the Michaelis–Menten equation to determine  $K_M$  and  $k_{cat}$ . (C) CB stain and anti-biotin WB analysis of AHA-containing PpaC-H6 and PpaC-H6GS3M4 with biotin alkyne. (D) Activity of PpaC immobilized on alkyne agarose resin. Each experiment was repeated three times. The average value and standard deviations are shown.

methionine, the addition of an ATG-encoding tag greatly improved the efficiency of modification.

Finally, we examined the usefulness of the AHA-containing tag in the immobilization of PpaC. PpaC-H6GS3M4 expressed in the presence of methionine or AHA was incubated with alkyne agarose resin for immobilization as described in [Materials and Methods](#). After immobilization, the resin was washed to remove free proteins, and the PpaC activity of proteins attached to the resin was measured ([Figure 4D](#)). For control, the alkyne agarose resin was incubated in the presence of bovine serum albumin (BSA). The activity of immobilized PpaC-H6GS3M4 was measured, as described in [Materials and Methods](#). Without AHA, there was a low level of adsorption of PpaC-H6GS3M4 to the agarose resin, leading to a low level of activity. When AHA was incorporated into the structure of PpaC, the level of activity increased approximately 8-fold, indicating more efficient immobilization. The control sample with BSA displayed no detectable activity.

In summary, we have shown that AHA-containing tags introduced at the C-terminus of two model proteins significantly increased the efficiency of the click chemistry reaction. The design of the tag is flexible. We tested three sequences, with two, three, or four extra ATG codons, in the tag. All of them significantly increased the level of labeling when the AHA-containing proteins were reacted with biotin alkyne. When combined with a polyhistidine tag, the histidine–AHA tag can facilitate both noncovalent interactions such as metal-affinity purification and covalent binding via reactions

with the alkyne functional group. We avoided the incorporation of multiple Met/AHA residues in a continuous stretch to avoid the potential problem of creating a hydrophobic patch, which may interfere with protein folding. Other than that, the design of the tag is really very flexible. The versatility of the tag design makes the concept broadly useful in the development of strategies to label and modify various proteins and immobilize proteins onto diverse alkyne-functionalized supporting matrices. A limitation of this method is the compatibility of the tag with specific protein structures. Although, in most cases, a short peptide tag as described in this study is not expected to drastically affect the structure and function of the protein of interest, there is always a possibility that certain proteins cannot tolerate such modifications.

## ■ MATERIALS AND METHODS

**Plasmid Construction.** Plasmids pET22-sfGFP and pET22-PpaC were created as described in earlier studies.<sup>45,46</sup> C-terminal tags were introduced via the fast cloning method using pET22-sfGFP or pET22-PpaC as the template, and primers are listed in [Table 1](#).<sup>47</sup> All coding sequences were confirmed through DNA sequencing.

**AHA Incorporation into Target Protein.** For protein expression, the corresponding plasmid was transformed into *E. coli* strain *DL41(DE3)*. Single colonies were first cultured overnight at 37 °C in M9 medium containing ampicillin (100 mg/L), and then the Met-starved overnight culture was used to inoculate 30 mL of fresh M9 medium containing 19 essential amino acids (each at 40 μg/mL without methionine) and 50 μg/mL of AHA with 10-fold dilution. The cells were grown at 37 °C with shaking at 250 rpm until its absorbance at 600 nm (OD<sub>600</sub>) reached 0.8, and then the cells were induced with 1 mM isopropyl-D-thiogalactopyranoside (IPTG). After overnight expression, the cells were harvested by centrifugation at 8000 rpm for 10 min. Cell pellets were stored at –80 °C. Control proteins with normal methionine in the tag were expressed the same as described except for replacing 50 μg/mL of AHA with 40 μg/mL of methionine in the culture medium.

**Protein Purification.** For purification, the cell pellet was resuspended in 30 mL of lysis buffer (50 mM 4-(2-hydroxyethyl)-1-piperazineethanesulfonic acid (HEPES), 200 mM NaCl, pH 7.5 for PpaC or 20 mM phosphate, 200 mM NaCl, pH 7.5 for sfGFP). The protease inhibitor phenylmethane sulfonyl fluoride was added freshly to a final concentration of 0.5 mM. The cells were lysed through sonication and then centrifuged at 10 000 rpm, 4 °C for 20 min. The supernatant was collected and incubated with Ni-NTA agarose beads (Qiagen) for 40 min at 4 °C with shaking. The resin was then loaded into an empty column, drained, and washed with the corresponding lysis buffer supplemented with 40 mM imidazole. Finally, proteins were eluted using the corresponding lysis buffer supplemented with 500 mM imidazole. After purification, imidazole in the samples was removed by dialysis against the lysis buffer.

**Bacteria Growth Curve.** *DL41(DE3)* strain was cultured overnight in M9 medium supplemented with 20 essential amino acids. The next morning, the overnight culture was used to inoculate three cultures of M9 medium supplemented with 19 essential amino acids (each at 40 μg/mL, no methionine) plus AHA (50 μg/mL), with 19 amino acids (each at 40 μg/mL, no methionine), or with all 20 essential amino acids (each at 40 μg/mL). Cell growth was measured by monitoring the

absorbance of the cell cultures at 600 nm (OD600) at the indicated time.

**Protein Biotinylation via Click Chemistry.** The reactivity of AHA residues in the structure of sfGFP and PpaC was examined through their reaction with PEG4 carboxamide-propargyl biotin (biotin alkyne). To initiate the reaction, biotin alkyne (50  $\mu\text{M}$ ), tris[(1-benzyl-1H-1,2,3-triazol-4-yl) methyl]-amine (TBTA, 600  $\mu\text{M}$ ), and CuBr (600  $\mu\text{M}$ ) were added into the purified protein sample in the HEPES buffer. The reaction mixture was incubated at room temperature with shaking for 5 min for sfGFP constructs and 1 h for PpaC constructs and then analyzed using anti-biotin WB.

**Protein Immobilization to Alkyne Agarose Resin.** Alkyne agarose resins were purchased from Jena Bioscience. The alkyne agarose beads were first washed with 10 bed volume of HEPES buffer (20 mM HEPES, 200 mM NaCl, pH 7.5) three times and then resuspended in 2 bed volume of HEPES buffer containing the indicated protein. TBTA was added to a final concentration of 600  $\mu\text{M}$  followed by mixing using a pipette tip. CuBr was then added to a final concentration of 200  $\mu\text{M}$ . The reaction mixture was mixed thoroughly using the pipette tip and incubated at room temperature for 2 h. Finally, the beads were washed using 10 bed volume of HEPES buffer via centrifugation three times.

**Gel Electrophoresis and WB.** Sodium dodecyl sulfate polyacrylamide gel electrophoresis (SDS-PAGE) was performed using 20% tris-glycine gel. For WB, proteins were transferred to a polyvinylidene fluoride membrane after SDS-PAGE and detected using a monoclonal anti-biotin antibody-alkaline phosphatase conjugate.

**Fluorescence Spectroscopy.** Fluorescence emission spectra were recorded using a PerkinElmer LS-55 fluorescence spectrometer (PerkinElmer, Waltham, MA) at 20 °C at an excitation wavelength of 485 nm.

Fluorescent images were taken using a fluorescence microscope (Nikon, Melville, NY).

**PpaC Activity Assay.** The PPase activity was measured using Mn pyrophosphate as the substrate as described.<sup>48</sup> Stock solutions of  $\text{MnCl}_2$  and sodium pyrophosphate were mixed at a 1:1 molar ratio at 0.5 mM right before the analysis (mixing an equal volume of 1.0 mM  $\text{MnCl}_2$  and 1.0 mM sodium pyrophosphate) and diluted to the indicated substrate concentration for the activity measurement. At neutral pH, pyrophosphate is not fully deprotonated. The major species is  $\text{MnH}_2\text{PPi}$  ( $\text{MnPPi}$ ), which was considered to be the substrate for PpaC.<sup>49</sup> A stock solution of malachite green (0.12%, w/v) was made by dissolving the dye in 3 M sulfuric acid. A working solution was always prepared fresh by adding one volume of 7.5% (w/v) ammonium molybdate into four volumes of the malachite green stock solution followed by the addition of Tween 20, to a final concentration of 0.2% (v/v). This solution is used to both terminate the enzyme reaction and initiate the colorimetric reaction to determine the concentration of phosphates. For activity measurements, PpaC was added into a freshly prepared reaction mixture containing the indicated concentration of  $\text{MnPPi}$ , in a reaction buffer (25 mM Tris-Cl, 50 mM NaCl, pH 7.0) at room temperature for 5 min. To terminate the enzymatic reaction and determine the phosphate concentration of a sample, one volume of the working solution was mixed with four volumes of the enzymatic reaction mixture to be analyzed. For immobilized PpaC, the reaction mixture was subjected to a quick centrifugation, and the supernatant was collected for analysis. The mixture was incubated for 5 min

for the color to develop, and the absorbance at 630 nm was measured. We have experimented with the conditions and confirmed that under these conditions, the product phosphate accumulation over time was linear. Therefore, the absorbance at 630 nm, after correction for background, directly correlates with the rate of hydrolysis. Michaelis–Menten constant  $K_M$  and specific enzymatic activity were determined through fitting the measured values using SigmaPlot.

## AUTHOR INFORMATION

### Corresponding Author

\*E-mail: [yinan.wei@uky.edu](mailto:yinan.wei@uky.edu). Phone: 859-257-7085. Fax: 859-323-1069 (Y.W.).

### ORCID

Yinan Wei: 0000-0002-9936-7149

### Notes

The authors declare no competing financial interest.

## ACKNOWLEDGMENTS

We would like to thank Drs. Jing Chen and Haining Zhu for their help with the mass spectroscopy peptide fingerprinting analysis. This work was supported by the Kentucky NSF EPSCoR RII Award 1355438 (to D.B. and Y.W.) and the Igniting Research Collaboration Award from the University of Kentucky (to Y.W.).

## REFERENCES

- (1) Smith, D. B.; Johnson, K. S. Single-step purification of polypeptides expressed in *Escherichia coli* as fusions with glutathione S-transferase. *Gene* **1988**, *67*, 31–40.
- (2) Zabel, U.; Häusler, C.; Weeger, M.; Schmidt, H. H. H. W. Homodimerization of soluble guanylyl cyclase subunits: Dimerization analysis using a glutathione-transferase affinity tag. *J. Biol. Chem.* **1999**, *274*, 18149–18152.
- (3) Schmidt, T. G. M.; Skerra, A. The random peptide library-assisted engineering of a C-terminal affinity peptide, useful for the detection and purification of a functional Ig Fv fragment. *Protein Eng.* **1993**, *6*, 109–122.
- (4) Skerra, A.; Schmidt, T. G. M. Use of the Strep-tag and streptavidin for detection and purification of recombinant proteins. *Methods Enzymol.* **2000**, *326*, 271–304.
- (5) Schmidt, T. G. M.; Skerra, A. The Strep-tag system for one-step purification and high-affinity detection or capturing of proteins. *Nat. Protoc.* **2007**, *2*, 1528–1535.
- (6) Green, N.; Alexander, H.; Olson, A.; Alexander, S.; Shinnick, T. M.; Sutcliffe, J. G.; Lerner, R. A. Immunogenic structure of the influenza virus hemagglutinin. *Cell* **1982**, *28*, 477–487.
- (7) Wang, Y.; Shao, Q.; Yu, X.; Kong, W.; Hildreth, J. E. K.; Liu, B. N-terminal hemagglutinin tag renders lysine-deficient APOBEC3G resistant to HIV-1 Vif-induced degradation by reduced polyubiquitination. *J. Virol.* **2011**, *85*, 4510–4519.
- (8) Hopp, T. P.; Prickett, K. S.; Price, V. L.; Libby, R. T.; March, C. J.; Cerretti, D. P.; Urdal, D. L.; Conlon, P. J. A short polypeptide marker sequence useful for recombinant protein identification and purification. *Bio/Technology* **1988**, *6*, 1204–1210.
- (9) Knappik, A.; Plückthun, A. An improved affinity tag based on the FLAG peptide for the detection and purification of recombinant antibody fragments. *BioTechniques* **1994**, *17*, 754–761.
- (10) Einhauer, A.; Jungbauer, A. The FLAG peptide, a versatile fusion tag for the purification of recombinant proteins. *J. Biochem. Biophys. Methods* **2001**, *49*, 455–465.
- (11) Sassenfeld, H. M.; Brewer, S. J. A polypeptide fusion designed for the purification of recombinant proteins. *Bio/Technology* **1984**, *2*, 76–81.

- (12) Nock, S.; Spudich, J. A.; Wagner, P. Reversible, site-specific immobilization of polyarginine-tagged fusion proteins on mica surfaces. *FEBS Lett.* **1997**, *414*, 233–238.
- (13) Evan, G. I.; Lewis, G. K.; Ramsay, G.; Bishop, J. M. Isolation of monoclonal antibodies specific for human *c-myc* proto-oncogene product. *Mol. Cell. Biol.* **1985**, *5*, 3610–3616.
- (14) Gottschling, D.; Seliger, H.; Tarrasón, G.; Piulats, J.; Eritja, R. Synthesis of oligodeoxynucleotides containing N<sup>4</sup>-mercaptoethylcytosine and their use in the preparation of oligonucleotide–peptide conjugates carrying *c-myc* tag-sequence. *Bioconjugate Chem.* **1998**, *9*, 831–837.
- (15) Hochuli, E.; Döbeli, H.; Schacher, A. New metal chelate adsorbent selective for proteins and peptides containing neighbouring histidine residues. *J. Chromatogr. A* **1987**, *411*, 177–184.
- (16) Honegger, A.; Mocikat, R.; Plückthun, A. Specific detection of his-tagged proteins with recombinant anti-His tag scFv-phosphatase or scFv-phage fusions. *BioTechniques* **1997**, *22*, 140–149.
- (17) Shah, N. H.; Muir, T. W. Inteins: Nature's gift to protein chemists. *Chem. Sci.* **2014**, *5*, 446–461.
- (18) Reddington, S. C.; Howarth, M. Secrets of a covalent interaction for biomaterials and biotechnology: SpyTag and SpyCatcher. *Curr. Opin. Chem. Biol.* **2015**, *29*, 94–99.
- (19) Zakeri, B.; Fierer, J. O.; Celik, E.; Chittock, E. C.; Schwarz-Linek, U.; Moy, V. T.; Howarth, M. Peptide tag forming a rapid covalent bond to a protein, through engineering a bacterial adhesin. *Proc. Natl. Acad. Sci. U.S.A.* **2012**, *109*, E690–E697.
- (20) Zakeri, B.; Howarth, M. Spontaneous intermolecular amide bond formation between side chains for irreversible peptide targeting. *J. Am. Chem. Soc.* **2010**, *132*, 4526–4527.
- (21) Wang, J.; Yu, Y.; Xia, J. Short peptide tag for covalent protein labeling based on coiled coils. *Bioconjugate Chem.* **2014**, *25*, 178–187.
- (22) Lai, Y.-T.; Chang, Y.-Y.; Hu, L.; Yang, Y.; Chao, A.; Du, Z.-Y.; Tanner, J. A.; Chye, M.-L.; Qian, C.; Ng, K.-M.; Li, H.; Sun, H. Rapid labeling of intracellular His-tagged proteins in living cells. *Proc. Natl. Acad. Sci. U.S.A.* **2015**, *112*, 2948–2953.
- (23) Uchinomiya, S.; Nonaka, H.; Wakayama, S.; Ojida, A.; Hamachi, I. In-cell covalent labeling of reactive His-tag fused proteins. *Chem. Commun.* **2013**, *49*, 5022–5024.
- (24) Uttamapinant, C.; White, K. A.; Baruah, H.; Thompson, S.; Fernández-Suárez, M.; Puthenveetil, S.; Ting, A. Y. A fluorophore ligase for site-specific protein labeling inside living cells. *Proc. Natl. Acad. Sci. U.S.A.* **2010**, *107*, 10914–10919.
- (25) Lin, C.-W.; Ting, A. Y. Transglutaminase-catalyzed site-specific conjugation of small-molecule probes to proteins in vitro and on the surface of living cells. *J. Am. Chem. Soc.* **2006**, *128*, 4542–4543.
- (26) Antos, J. M.; Chew, G.-L.; Guimaraes, C. P.; Yoder, N. C.; Grotenbreg, G. M.; Popp, M. W.-L.; Ploegh, H. L. Site-specific N- and C-terminal labeling of a single polypeptide using sortases of different specificity. *J. Am. Chem. Soc.* **2009**, *131*, 10800–10801.
- (27) Carrico, I. S.; Carlson, B. L.; Bertozzi, C. R. Introducing genetically encoded aldehydes into proteins. *Nat. Chem. Biol.* **2007**, *3*, 321–322.
- (28) Zhou, Z.; Cironi, P.; Lin, A. J.; Xu, Y.; Hrvatin, S.; Golan, D. E.; Silver, P. A.; Walsh, C. T.; Yin, J. Genetically encoded short peptide tags for orthogonal protein labeling by Sfp and AcpS phosphopantetheinyl transferases. *ACS Chem. Biol.* **2007**, *2*, 337–346.
- (29) Kiick, K. L.; Saxon, E.; Tirrell, D. A.; Bertozzi, C. R. Incorporation of azides into recombinant proteins for chemoselective modification by the Staudinger ligation. *Proc. Natl. Acad. Sci. U.S.A.* **2002**, *99*, 19–24.
- (30) Lang, K.; Davis, L.; Torres-Kolbus, J.; Chou, C.; Deiters, A.; Chin, J. W. Genetically encoded norbornene directs site-specific cellular protein labelling via a rapid bioorthogonal reaction. *Nat. Chem.* **2012**, *4*, 298–304.
- (31) Chin, J. W.; Santoro, S. W.; Martin, A. B.; King, D. S.; Wang, L.; Schultz, P. G. Addition of *p*-Azido-L-phenylalanine to the Genetic Code of *Escherichia coli*. *J. Am. Chem. Soc.* **2002**, *124*, 9026–9027.
- (32) Exner, M. P.; Kuenzl, T.; To, T. M. T.; Ouyang, Z.; Schwagerus, S.; Hoesl, M. G.; Hackenberger, C. P. R.; Lensen, M. C.; Panke, S.; Budisa, N. Design of S-Allylcysteine in Situ Production and Incorporation Based on a Novel Pyrrolysyl-tRNA Synthetase Variant. *ChemBioChem* **2017**, *18*, 85–90.
- (33) Kramer, G.; Kasper, P. T.; de Jong, L.; de Koster, C. G. Quantitation of newly synthesized proteins by pulse labeling with azidohomoalanine. *Methods Mol. Biol.* **2011**, *753*, 169–181.
- (34) Martell, J.; Weerapana, E. Applications of copper-catalyzed click chemistry in activity-based protein profiling. *Molecules* **2014**, *19*, 1378–1393.
- (35) Avti, P. K.; Maysinger, D.; Kakkar, A. Alkyne-azide “click” chemistry in designing nanocarriers for applications in biology. *Molecules* **2013**, *18*, 9531–9549.
- (36) Hatzenpichler, R.; Scheller, S.; Tavormina, P. L.; Babin, B. M.; Tirrell, D. A.; Orphan, V. J. In situ visualization of newly synthesized proteins in environmental microbes using amino acid tagging and click chemistry. *Environ. Microbiol.* **2014**, *16*, 2568–2590.
- (37) tom Dieck, S.; Kochen, L.; Hanus, C.; Heumüller, M.; Bartnik, I.; Nassim-Assir, B.; Merk, K.; Mosler, T.; Garg, S.; Bunse, S.; Tirrell, D. A.; Schuman, E. M. Direct visualization of newly synthesized target proteins in situ. *Nat. Methods* **2015**, *12*, 411–414.
- (38) Link, A. J.; Tirrell, D. A. Cell Surface Labeling of *Escherichia coli* via Copper(I)-Catalyzed [3 + 2] Cycloaddition. *J. Am. Chem. Soc.* **2003**, *125*, 11164–11165.
- (39) Simon, M.; Stefan, N.; Borsig, L.; Plückthun, A.; Zangemeister-Wittke, U. Increasing the antitumor effect of an EpCAM-targeting fusion toxin by facile click PEGylation. *Mol. Cancer Ther.* **2014**, *13*, 375–385.
- (40) McClatchy, D. B.; Ma, Y.; Liu, C.; Stein, B. D.; Martínez-Bartolomé, S.; Vasquez, D.; Hellberg, K.; Shaw, R. J.; Yates, J. R., III Pulsed Azidohomoalanine Labeling in Mammals (PALM) Detects Changes in Liver-Specific LKB1 Knockout Mice. *J. Proteome Res.* **2015**, *14*, 4815–4822.
- (41) Dieterich, D. C.; Hodas, J. J. L.; Gouzer, G.; Shadrin, I. Y.; Ngo, J. T.; Triller, A.; Tirrell, D. A.; Schuman, E. M. In situ visualization and dynamics of newly synthesized proteins in rat hippocampal neurons. *Nat. Neurosci.* **2010**, *13*, 897–905.
- (42) Deal, R. B.; Henikoff, J. G.; Henikoff, S. Genome-wide kinetics of nucleosome turnover determined by metabolic labeling of histones. *Science* **2010**, *328*, 1161–1164.
- (43) Ma, Y.; Biava, H.; Contestabile, R.; Budisa, N.; di Salvo, M. Coupling bioorthogonal chemistries with artificial metabolism: Intracellular biosynthesis of azidohomoalanine and its incorporation into recombinant proteins. *Molecules* **2014**, *19*, 1004–1022.
- (44) Agard, N. J.; Baskin, J. M.; Prescher, J. A.; Lo, A.; Bertozzi, C. R. A comparative study of bioorthogonal reactions with azides. *ACS Chem. Biol.* **2006**, *1*, 644–648.
- (45) Gajadeera, C. S.; Zhang, X.; Wei, Y.; Tsodikov, O. V. Structure of inorganic pyrophosphatase from *Staphylococcus aureus* reveals conformational flexibility of the active site. *J. Struct. Biol.* **2015**, *189*, 81–86.
- (46) Zhong, M.; Fang, J.; Wei, Y. Site specific and reversible protein immobilization facilitated by a DNA binding fusion tag. *Bioconjugate Chem.* **2010**, *21*, 1177–1182.
- (47) Li, C.; Wen, A.; Shen, B.; Lu, J.; Huang, Y.; Chang, Y. FastCloning: A highly simplified, purification-free, sequence- and ligation-independent PCR cloning method. *BMC Biotechnol.* **2011**, *11*, 92.
- (48) Baykov, A. A.; Evtushenko, O. A.; Avaeva, S. M. A malachite green procedure for orthophosphate determination and its use in alkaline phosphatase-based enzyme immunoassay. *Anal. Biochem.* **1988**, *171*, 266–270.
- (49) Lahti, R.; Jokinen, M. Kinetic model for the action of the inorganic pyrophosphatase from *Streptococcus faecalis*. *Biochemistry* **1985**, *24*, 3526–3530.
- (50) Bundy, B. C.; Swartz, J. R. Site-specific incorporation of *p*-propargyloxyphenylalanine in a cell-free environment for direct protein–protein click conjugation. *Bioconjugate Chem.* **2010**, *21*, 255–263.

(51) Pédelacq, J.-D.; Cabantous, S.; Tran, T.; Terwilliger, T. C.; Waldo, G. S. Engineering and characterization of a superfolder green fluorescent protein. *Nat. Biotechnol.* **2006**, *24*, 79–88.